Role of resonances in $\rho^0 \to \pi^+\pi^-\gamma$

G. Toledo Sánchez

Instituto de Física, Universidad Nacional Autónoma de México, México D. F. C. P. 04510

J. L. García-Luna and V. González-Enciso

Departamento de Física, Centro Universitario de Ciencias Exactas e Ingenierías, Universidad de Guadalajara, Boulevard Marcelino García Barragán 1508, C. P. 44840, Guadalajara, Jalisco, México

(Received 15 March 2007; published 6 August 2007)

We study the effect of the $\sigma(600)$ and $a_1(1260)$ resonances in the $\rho^0 \to \pi^+\pi^-\gamma$ decay within the meson dominance model. Major effects are driven by the mass and width parameters of the $\sigma(600)$, and the usually neglected contribution of the $a_1(1260)$, although small by itself, may become sizable through its interference with pion bremsstrahlung, and the proper relative sign can favor the central value of the experimental branching ratio. We present a procedure, using the gauge invariant structure of the resonant amplitudes, to kinematically enhance the resonant effects in the angular and energy distribution of the photon. We also elaborate on the coupling constants involved.

DOI: 10.1103/PhysRevD.76.033001 PACS numbers: 13.40.Hq, 12.20.Ds, 12.40.Vv

I. INTRODUCTION

The ρ^0 meson can be produced via e^+e^- annihilation. Dedicated experiments like KLOE, SND, and CMD-II have performed extensive studies on the decay modes of this meson [1–4]. The measured branching ratio of the $\rho^0 \to \pi^+\pi^-\gamma$ radiative decay is $9.9 \pm 1.6 \times 10^{-3}$ [1]. The theoretical approach is able to explain the experimental result, at the current precision, considering the radiation off pions alone. This can be estimated in a model independent way, predicting a branching ratio around 1 standard deviation above the central value [5–7]. The maximum energy that the photon can carry out in this process is $\omega = 334.8$ MeV, which is large enough to suggest that contributions beyond the soft photon approximation may be relevant in future accurate measurements.

The introduction of the subleading contributions is model dependent. If the scalar contribution is identified with the $\sigma(600)$ resonance then both mass and width may be obtained by making a fit to the data. Still, the range of values obtained using this procedure is not as precise as the determination from other methods [8,9]. The other allowed contribution for the decay is of the axial-vector form. The coupling of the relevant amplitude is estimated in the chiral perturbation theory to be proportional to the parameters $L_9^r + L_{10}^r \simeq 1.4 \times 10^{-3}$, and therefore is commonly disregarded in the analysis [7]. On the other hand, meson dominance identifies this contribution with the $a_1(1260)$ state which, at first, is far from being on shell and then is not taken into account.

The improvement of the experimental precision will make it possible to distinguish the resonant contributions, and therefore a clear theoretical estimate will be important. In particular, we can ask whether such contributions can help to bring the theoretical predictions closer to the central experimental value and if there is a window where the resonant contributions are more relevant. The quark structure and proper characterization of such states is also a matter of ongoing research [11–13].

In this article we use the meson dominance model to provide a full account of these resonances. We perform a self-consistent determination of the effective coupling constants involved by reproducing observables in other decays without invoking the one-loop corrections. Since the radiation is dominated by pion bremsstrahlung, the resonant contribution upon its interference with the pion bremsstrahlung can become relevant. Here we compute the contributions to the branching ratio from the different sources which may also provide a hint to the relative sign of the $a_1(1260)$ amplitude by favoring the experimental central value. The di-pion invariant mass spectrum and the angular and energy distribution of the photon are used to look for sensitivity to the resonances. We exploit kinematical configurations which for the latter may lead to enhancements of the resonant contributions. The $\sigma(600)$ mass and width effects are explored throughout the analysis.

II. DECAY AMPLITUDES

Let us state the conventions for the process $\rho^0(q, \eta) \to \pi^+(p')\pi^-(p)\gamma(k, \epsilon)$; q, p', p, and k are the corresponding 4-momenta, and η and ϵ are the polarization tensors of the vector meson and the photon, respectively. The Feynman diagrams contributing to the decay are shown in Fig. 1. Figures 1(a)–1(c) are model independent and correspond to the Low amplitude [14]. Figures 1(d)–1(f) are model dependent and, in the meson dominance model, include the intermediate σ and a_1 resonances. We will use the dependence on these states to label the corresponding amplitudes. The intermediate state $f(980)$ is not taken into account since it is considered to be dominated by the KK channel [13]. Therefore, the total amplitude can be written as

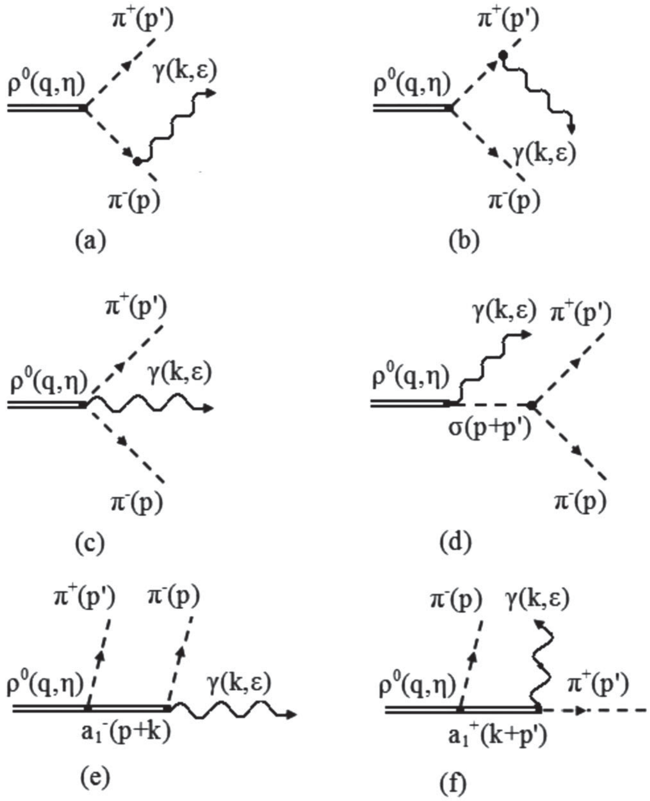

FIG. 1. Feynman diagrams that contribute to the decay $\rho^0 \to \pi^+\pi^-\gamma$.

$$\mathcal{M}_T = \mathcal{M}_L + \mathcal{M}_\sigma + \mathcal{M}_{a_1^+} + \mathcal{M}_{a_1^-}, \tag{1}$$

where the Low amplitude [5], $\mathcal{M}_L = \mathcal{M}_a + \mathcal{M}_b + \mathcal{M}_c$, can be split into two parts, owing to its dependence on the photon energy: $\mathcal{M}_L = \mathcal{M}_e(\omega^{-1}) + \mathcal{M}_0(\omega^0)$, where

$$\mathcal{M}_e = 2ieg_{\rho\pi\pi} p' \cdot \eta L \cdot \epsilon^*, \tag{2}$$

$$\mathcal{M}_0 = 2ieg_{\rho\pi\pi}\left[\epsilon^* \cdot \eta - \frac{p' \cdot \epsilon^* k \cdot \eta}{p' \cdot k}\right], \tag{3}$$

and $L^\nu = p^\nu/p \cdot k - p'^\nu/p' \cdot k$ satisfies $L \cdot k = 0$. Therefore, M_L is explicitly gauge invariant. $g_{\rho\pi\pi}$ is the coupling constant between the rho and the pions, as indicated by the subindex. The amplitudes for Figs. 1(d)–1(f) are gauge invariant by themselves and are given by

$$\mathcal{M}_\sigma = -ieg_{\rho\sigma\gamma}g_{\sigma\pi\pi}\left[\frac{q \cdot k\epsilon^* \cdot \eta - q \cdot \epsilon^* k \cdot \eta}{(p+p')^2 - m_\sigma^2 + im_\sigma\Gamma_\sigma}\right], \tag{4}$$

$$\mathcal{M}_{a_1^+} = \frac{ig_{a_1\pi\gamma}g_{a_1\rho\pi}p' \cdot k(k+p') \cdot q}{(k+p')^2 - m_{a_1}^2 + im_{a_1}\Gamma_{a_1}}\epsilon^{*\lambda}\eta^\theta\left(-g^{\nu\lambda} + \frac{p'^\lambda k^\nu}{p' \cdot k}\right) \times \left(g^{\theta\nu} - \frac{(k+p')^\theta q^\nu}{(k+p') \cdot q}\right), \tag{5}$$

$$\mathcal{M}_{a_1^-} = \frac{ig_{a_1\pi\gamma}g_{a_1\rho\pi}p \cdot k(k+p) \cdot q}{(k+p)^2 - m_{a_1}^2 + im_{a_1}\Gamma_{a_1}}\epsilon^{*\lambda}\eta^\theta\left(-g^{\nu\lambda} + \frac{p^\lambda k^\nu}{p \cdot k}\right) \times \left(g^{\theta\nu} - \frac{(k+p)^\theta q^\nu}{(k+p) \cdot q}\right), \tag{6}$$

respectively, where $g_{\sigma\pi\pi}$, $g_{a_1\pi\gamma}$, and $g_{a_1\rho\pi}$ are effective coupling constants. m_σ (Γ_σ) and m_{a_1} (Γ_{a_1}) are the corresponding particle masses (full widths). The resonant propagators have been assumed to be of the complex mass form [15], which corresponds to replacing $m^2 \to m^2 - im\Gamma$ in the nonresonant propagator.

III. SQUARED AMPLITUDES AND INTERFERENCES

We choose $p \cdot k$ and $p' \cdot k$ as the independent variables to make the dependence on the photon energy explicit. We list below some of the relevant squared amplitudes and interferences:

$$|\mathcal{M}_e|^2 = 16\pi\alpha g_{\rho\pi\pi}^2 L^2\left(m_\pi^2 - \frac{M_\rho^2}{4} - \frac{(p \cdot k)^2}{M_\rho^2}\right), \tag{7}$$

$$|\mathcal{M}_0|^2 = 16\pi\alpha g_{\rho\pi\pi}^2\left(1 + \frac{(p \cdot k + p' \cdot k)}{M_\rho^2 p' \cdot k} \times \left(M_\rho^2 - m_\pi^2 - \frac{p \cdot k m_\pi^2}{p' \cdot k} - 2p \cdot k\right)\right), \tag{8}$$

$$2\,\mathrm{Re}\mathcal{M}_e\mathcal{M}_\sigma^\dagger = 16\pi\alpha g_{\rho\pi\pi}g_{\rho\sigma\gamma}g_{\sigma\pi\pi}p \cdot kp' \cdot kL^2 \times \left(\frac{M_\rho^2 - m_\sigma^2 - 2q \cdot k}{[M_\rho^2 - m_\sigma^2 - 2q \cdot k]^2 + m_\sigma^2\Gamma_\sigma^2}\right), \tag{9}$$

$$2\,\mathrm{Re}\mathcal{M}_e\mathcal{M}_{a_1^+}^\dagger = 4eg_{\rho\pi\pi}g_{a_1\pi\gamma}g_{a_1\rho\pi}p \cdot kp' \cdot kL^2 \times \left(\frac{[m_\pi^2 + p' \cdot k][m_\pi^2 - m_{a1}^2 + 2p' \cdot k]}{[m_\pi^2 + 2p' \cdot k - m_{a1}^2]^2 + m_{a1}^2\Gamma_{a1}^2}\right), \tag{10}$$

$$2\,\mathrm{Re}\mathcal{M}_e\mathcal{M}_{a_1^-}^\dagger = 4eg_{\rho\pi\pi}g_{a_1\pi\gamma}g_{a_1\rho\pi}p \cdot kp' \cdot kL^2 \times \left(\frac{[m_\pi^2 + 2p \cdot k][m_\pi^2 - m_{a1}^2 + 2p \cdot k]}{[m_\pi^2 + 2p \cdot k - m_{a1}^2]^2 + m_{a1}^2\Gamma_{a1}^2}\right). \tag{11}$$

We have not written the square of the model dependent amplitudes and the remaining interferences, but they are actually taken into account in the calculation. The Low interferences of order ω^{-1} are null in accordance with the Burnett-Kroll theorem [16], and a term proportional to L^2 from the $\mathcal{M}_e\mathcal{M}_0^\dagger$ interference was absorbed into Eq. (7). By inspection of Eqs. (7)–(11) we observe that, in addition to $|\mathcal{M}_e|^2$, all the interferences are proportional to L^2, a property we showed in a previous work to hold whenever there is an interference between the electric charge radiation and any gauge invariant amplitude [17]. This property will allow us to kinematically enhance the model dependent contribution by properly choosing the region where L^2 is maximum [18]. Although this enhancement is also promoted to the dominant electric charge contribution, the latter receives a natural suppression as the photon energy increases, owing to the ω^{-2} dependence, while the model dependent ones are of order ω^0 and higher.

IV. RESULTS

In order to make an estimate of the observables, we first address the problem of finding the proper values of the coupling constants. The $g_{\rho\pi\pi}$ and $g_{\sigma\pi\pi}$ couplings can be written in terms of masses and widths as

$$g^2_{\rho\pi\pi} = \frac{48\pi\Gamma_\rho}{M_\rho}\left(1 - \frac{4m^2_\pi}{M^2_\rho}\right)^{-3/2} = (6.01)^2, \tag{12}$$

$$g^2_{\sigma\pi\pi} = \frac{32\pi\Gamma_\sigma m_\sigma}{3\sqrt{1-\frac{4m^2_\pi}{m^2_\sigma}}}, \tag{13}$$

where we have used for definiteness $\Gamma_\rho = 150.7$ MeV and $M_\rho = 775$ MeV. For the $g_{\rho\sigma\gamma}$ coupling, we use the expression depending on the radiative width $\Gamma_{\rho\sigma\gamma}$, whose value was estimated to be $\Gamma_{\rho\sigma\gamma} = 0.23 \pm 0.47$ keV or 17 ± 4 keV [19]:

$$g^2_{\rho\sigma\gamma} = \frac{3}{\alpha}\Gamma_{\rho\sigma\gamma}\left(\frac{2M_\rho}{M^2_\rho - m^2_\sigma}\right)^3. \tag{14}$$

Taking the prediction for $\Gamma_{\rho\sigma\gamma} = 17 \pm 4$ keV and varying $m_\sigma = 350$–500 MeV produces $g^2_{\rho\sigma\gamma} = (1.82$–$7.46) \times 10^{-7}$ MeV^{-2}. To compare with the one obtained in [20] we reparametrize the coupling by an M_ρ factor ($g_{\rho\sigma\gamma} \to \hat{g}_{\rho\sigma\gamma} = M_\rho g_{\rho\sigma\gamma} \to 0.33$–$0.67$). Therefore, it is 1 order of magnitude smaller than the one extracted in [20] which lies in the region of |6–7|, and produces an overestimate of the branching ratio for $\rho^0 \to \sigma\pi \to \pi^0\pi^0\gamma$ [21]. Our Eq. (14) is valid in the limit of $\Gamma_\sigma = 0$. In Ref. [22] the coupling was computed including the width effect and relying on the experimental value for $\Gamma(\rho^0 \to \sigma\pi \to \pi^0\pi^0\gamma) = (2.9^{+1.4}_{-1.2} \pm 0.6)$ keV [3]. Using their master equation and varying m_σ and Γ_σ from 350–500 MeV produces $\hat{g}_{\rho\sigma\gamma} = 0.22$–$0.89$, which is of the same order as our value, although in a different approximation. Therefore, the use of either value will produce similar results in the range we are exploring. An estimate of the $g_{a_1\rho\pi}$ coupling can be obtained from the $a_1(q, \eta) \to \rho(k, \epsilon)\pi$ decay. The amplitude in its simplest on shell form becomes [23]

$$\mathcal{M}(a_1 \to \rho\pi) = f_{a_1\rho\pi}\left(\eta \cdot \epsilon^* - k \cdot \eta \frac{q \cdot \epsilon^*}{k \cdot q}\right). \tag{15}$$

Our coupling is related to this by $g_{a_1\rho\pi} = -f_{a_1\rho\pi}/k \cdot q$. Assuming that the full width is dominated by the $\rho\pi$ channel, the coupling is

$$f^2_{a_1\rho\pi} = \frac{12\pi m^3_{a_1}\Gamma_{a_1}}{[\rho^-\pi^0] + [\rho^0\pi^-]} = (3.7\text{–}5.9\ \text{GeV})^2, \tag{16}$$

where $[\rho\pi] \equiv [1 + M^2_\rho m^2_{a_1}/(2(k \cdot q)^2)]\sqrt{(k\cdot q)^2 - M^2_\rho m^2_{a_1}}$ and $k \cdot q = (m^2_{a_1} + M^2_\rho - m^2_\pi)/2$, and we have used $m^2_{a_1} = 1230 \pm 40$ and $\Gamma_{a_1} = 250$–600 MeV. This compares well with the prediction of $f_{a_1\rho\pi} = 4.8$ GeV in the quark model [23]. Finally, using vector meson dominance arguments [24], we can relate the $g_{a_1\rho\pi}$ and $g_{a_1\pi\gamma}$ as follows: $g_{a_1\pi\gamma} = eg_{a_1\rho\pi}/\gamma_\rho$, where $\gamma_\rho = 2\alpha\sqrt{\pi M_\rho/3\Gamma(\rho^0 \to e^+e^-)} = 5.012$. Errors in the observables coming from the uncertainties on the coupling values will be specified below.

The radiative decay width can be computed using the expressions for the squared amplitudes and interferences separately. In Table I, we present the different contributions to the branching ratio for a set of values for the mass and width of the $\sigma(600)$. We have introduced a 50 MeV cut in the photon energy to avoid the infrared divergence; then its allowed region is $\omega_{\text{cut}} \leq \omega \leq (M^2_\rho - 4m^2_\pi)/2M_\rho = 334.8$ MeV. The upper value requires going beyond the soft photon approximation, given by the Low amplitude. It is worth mentioning that the higher the cut in the photon energy, the better the sensitivity to the resonant parameters. Here we stick to this value to compare with the available data. The Low amplitude contribution to the branching ratio is Low $= 11.547 \times 10^{-3}$, about 1 standard deviation above the experimental value of $9.9 \pm 1.6 \times 10^{-3}$ [1], for the same cutoff. The column labeled "Sigma" corresponds to the contribution from the σ amplitude itself and its interference with the Low amplitude. This becomes larger for smaller values of the σ parameters and can even flip the sign. The column labeled "Low + σ" is the sum of the previous column plus the Low contribution. The columns labeled "Tot(+)" and "Tot(−)" correspond to the total branching ratio when the a_1 interference with the Low amplitude is also included. Depending on the sign of the a_1 amplitudes, the contribution can be either $a_1(+) = 6.8 \times 10^{-5}$ or $a_1(-) = -6.6 \times 10^{-5}$.

From Table I, we observe that the inclusion of the resonances can help to bring the prediction closer to the central experimental value. In particular the sign on the a_1 amplitude can either improve or worsen the agreement. Still, the major effect is driven only by the m_σ and Γ_σ parameters. To have an idea of the effect from the uncertainties in the coupling constants discussed previously and a_1 mass and width, we have included error bars in the first and last row of Table I. The contributions from a_1 itself is of the order of 10^{-6} and neglected in the results.

The di-pion invariant mass is interesting on its own and the experiments usually report it as the main observable. However, in our case the individual effects from the interferences between the electric radiation and the resonances are very mild, as can be expected from the results for the

TABLE I. Branching ratios from several contributions for a set of values of the σ parameters and a cutoff on the photon energy of 50 MeV. Low $= 11.547 \times 10^{-3}$. To have an idea of the effect from the uncertainties in the coupling constants and a_1 mass and width, we have included error bars in the first and last rows. See text for details.

M_σ (MeV)	Γ_σ (MeV)	Sigma (10^{-5})	Low + σ (10^{-3})	Tot. (+) (10^{-3})	Tot. (-) (10^{-3})
500	500	1.7	11.56	11.64 ± 0.03	11.49 ± 0.01
500	450	2.0	11.57	11.64	11.50
500	400	2.4	11.57	11.64	11.50
500	350	2.9	11.58	11.65	11.50
450	500	−5.8	11.49	11.56	11.42
450	450	−6.1	11.49	11.56	11.42
450	400	−6.4	11.48	11.55	11.41
450	350	−6.5	11.48	11.50	11.41
400	500	−11.7	11.43	11.49	11.36
400	450	−12.4	11.42	11.49	11.35
400	400	−13.0	11.42	11.49	11.35
400	350	−13.7	11.41	11.48	11.34
350	500	−17.0	11.38	11.45	11.31
350	450	−17.9	11.37	11.44	11.30
350	400	−18.8	11.36	11.43	11.29
350	350	−19.7	11.35	11.42 ± 0.05	11.28 ± 0.07

branching ratios. Just for illustration, in Fig. 2 we plot the corresponding Low amplitude, which dominates this observable.

The fact that all the leading interferences are proportional to L^2 allows us to look for an enhancement of the effects from the resonances by choosing the kinematical configuration where L^2 is maximum. In the ρ^0 restframe it can be written as $L^2 \propto 1 - \cos^2\theta$, where θ is the angle between the photon and π^- 3-momenta. In addition, the dependence on the photon energy of the interferences is of order ω^0 while the dominant Low contribution is of order ω^{-2}. This suggests that an appropriate observable could be the angular and energy distribution of the photon

$$d\Gamma = \sum_{E=E^+,E^-} \frac{|\bar{\mathcal{M}}|^2}{(2\pi)^5} \frac{M_\rho}{8} \frac{\sqrt{E^2 - m_\pi^2}}{|F'(E)|} x dx dy, \qquad (17)$$

where $E^\pm$ labels the roots of $F(E) = M_\rho^2 - 2M_\rho E - 2M_\rho \omega + 2(E\omega - p\omega\cos\theta)$ in the ρ^0 restframe, and we have introduced the dimensionless variables $y \equiv \cos\theta$ and $x \equiv \omega/M_\rho$. The maximum value for ω is $(M_\rho^2 - 2m_\pi M_\rho)/2(M_\rho - m_\pi)$. In Figs. 3–5 we plot $d\Gamma/\Gamma_{nr} dy dx$ (normalized to the nonradiative width, Γ_{nr}) for two angles of the photon emission, $\theta = 85°$ and $5°$ (solid and dashed lines, respectively). Figure 3 includes the Low contribution, Fig. 4 the interference between Low and σ, and Fig. 5 the interference between Low and a_1 emission. Here we have used $m_\sigma = \Gamma_\sigma = 400$ MeV. We can observe that, although small, the contributions from the resonances can be strongly enhanced by choosing the proper angle of emission, about 50% for the σ and up to 85% for the a_1 in the current setup of relative angles. This enhancement is not promoted to the Low emission at the same proportion, which is mildly affected and even suppressed for large

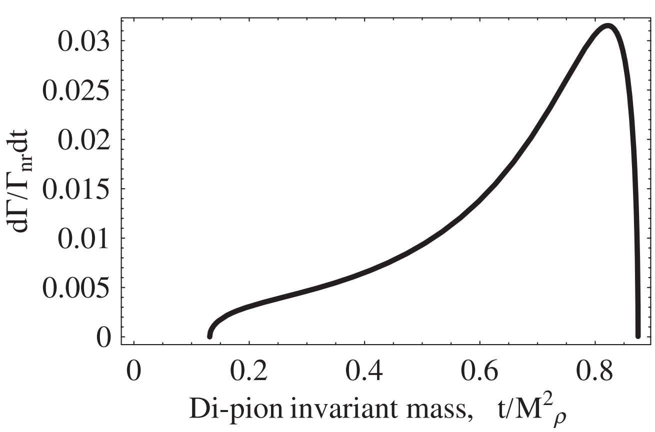

FIG. 2. Di-pion invariant mass due to the pion bremsstrahlung for the $\rho^0 \to \pi^+\pi^-\gamma$ decay.

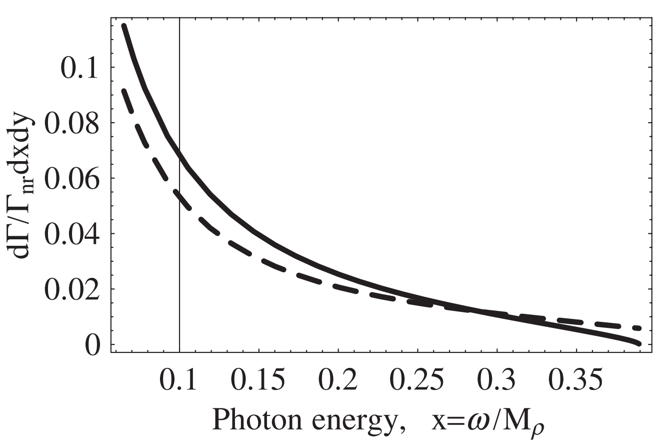

FIG. 3. Photon energy spectrum due to the Low emission for $\theta = 85°$ and $5°$ (solid and dashed lines, respectively).

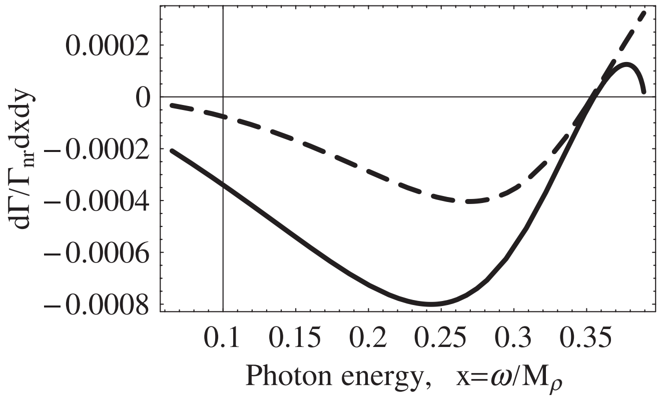

FIG. 4. Photon energy spectrum due to the interference between electric and σ emission for $\theta = 85°$ and $5°$ (solid and dashed lines, respectively). Here $m_\sigma = \Gamma_\sigma = 400$ MeV.

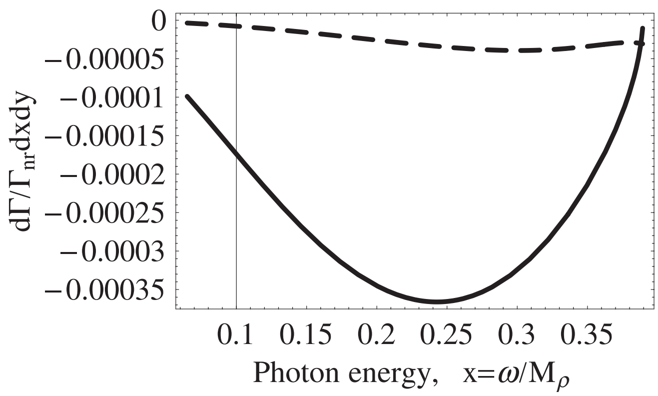

FIG. 5. Photon energy spectrum due to the interference between electric and a_1 emission for $\theta = 85°$ and $5°$ (solid and dashed lines, respectively).

values of the photon energy as expected (Fig. 3). The total photon energy and angular spectrum is certainly dominated by the Low emission, but this is free of relevant theoretical uncertainties and can be safely removed from data.

V. CONCLUSIONS

We have studied the $\rho^0 \longrightarrow \pi^+\pi^-\gamma$ decay in a self-consistent approach based on the meson dominance model, and included both the $\sigma(600)$ and $a_1(1260)$ resonances. We determined the corresponding coupling constants involved, and, in particular, the value for $g_{\rho\sigma\gamma}$ is 1 order of magnitude smaller than the one extracted in previous studies [20] but similar to the estimation made in [22] for the particular range of parameters we did explore. Rigorously, one must use the coupling from the latter where Γ_σ is taken into account.

We identified the different contributions to the branching ratio, dominated by the pion bremsstrahlung whose contribution alone lies 1 standard deviation above the experimental central value (measured with a precision of about 16%). The resonant contributions upon interference with the Low radiation, although small, can be of relevance for future accurate measurements of the branching ratio and be sensitive to the resonance parameters. In fact, this would provide a hint on the relative sign of the axial amplitudes by requiring the theoretical prediction to lie closer to the central experimental value. In order to distinguish the effects coming from the $\sigma(600)$ parameters a precision smaller than 5% is required, while to be sensitive to the a_1 parameters at least the 1% level is required.

On the other hand, the di-pion invariant mass spectrum was computed and shown to be saturated by the pion bremsstrahlung.

Exploiting the structure of the leading interferences, we tuned a kinematical configuration where resonant contributions can be enhanced, namely, the photon angular and energy spectrum. In particular, the effects can be enhanced for quasitransversal emission compared to quasicollinear emission of photons, with respect to the π^- 3-momentum. Our treatment is useful for looking for enhancements of the resonances in decays of the form $\rho^0 \to \pi^+\pi^-\gamma$, since it exploits the radiation structure of the external charged particles and can serve as a complement to estimates from decays of the form $\rho^0 \to \pi^0\pi^0\gamma$, which are mainly driven by model dependent contributions, and where charged particles contribute only through loops, and therefore our approach can not be applied.

ACKNOWLEDGMENTS

We are grateful to G. López Castro and Jens Erler for very useful observations. This work was partially supported by Conacyt México, under Grant No. 42026-F.

[1] S. I. Dolinsky *et al.*, Phys. Rep. **202**, 99 (1991).
[2] M. N. Achasov *et al.*, Phys. Lett. B **537**, 201 (2002).
[3] A. Aloisio *et al.*, Phys. Lett. B **606**, 12 (2005); R. R. Akhmetshin *et al.*, Phys. Lett. B **578**, 285 (2004).
[4] W.-M. Yao *et al.*, J. Phys. G **33**, 1 (2006).
[5] P. Singer, Phys. Rev. **130**, 2441 (1963); **161**, 1694(E) (1967).
[6] A. Bramon, G. Colangelo, P. J. Franzini, and M. Greco, Phys. Lett. B **287**, 263 (1992); K. Huber and H. Neufeld, Phys. Lett. B **357**, 221 (1995); E. Marco, S. Hirenzaki, E. Oset, and H. Toki, Phys. Lett. B **470**, 20 (1999).
[7] A. Bramon and R. Escribano, J. High Energy Phys. 02 (2004) 048.
[8] See, for example, I. Caprini, G. Colangelo, and H.

Leutwyler, Phys. Rev. Lett. **96**, 132001 (2006), and references therein.
[9] E. M. Aitala *et al.* (E791 Collaboration), Phys. Rev. Lett. **86**, 770 (2001).
[10] G. Ecker, J. Gasser, and A. Pich, Nucl. Phys. **B321**, 311 (1989).
[11] J. R. Peláez and G. Rios, Phys. Rev. Lett. **97**, 242002 (2006), and references therein.
[12] J. A. Dankowych *et al.*, Phys. Rev. Lett. **46**, 580 (1981); W. Ruckstuhl *et al.* (DELCO Collaboration), Phys. Rev. Lett. **56**, 2132 (1986); D. M. Asner *et al.* (CLEO Collaboration), Phys. Rev. D **61**, 012002 (1999).
[13] See, for example, F. E. Close and N. A. Tornqvist, J. Phys. G **28**, R249 (2002); N. N. Achasov, V. V. Gubin, and E. P. Solodov, Phys. Rev. D **55**, 2672 (1997).
[14] F. E. Low, Phys. Rev. **110**, 974 (1958).
[15] G. López Castro, J. L. Lucio, and J. Pestieau, Int. J. Mod. Phys. A **11**, 563 (1996).
[16] T. H. Burnett and N. M. Kroll, Phys. Rev. Lett. **20**, 86 (1968).
[17] G. López Castro and G. Toledo Sánchez, J. Phys. G **27**, 2203 (2001).
[18] G. Toledo Sánchez, Phys. Rev. D **66**, 097301 (2002).
[19] D. Black, M. Harada, and J. Schechter, Phys. Rev. Lett. **88**, 181603 (2002).
[20] A. Gokalp and O. Yilmaz, Phys. Rev. D **62**, 093018 (2000).
[21] A. Gokalp, S. Solmaz, and O. Yilmaz, Phys. Rev. D **67**, 073007 (2003).
[22] M. K. Rekalo and E. Tomasi-Gustafsson, Nucl. Phys. **A725**, 116 (2003).
[23] N. Isgur, C. Morningstar, and C. Reader, Phys. Rev. D **39**, 1357 (1989).
[24] M. Gell-Mann, D. Sharp, and W. G. Wagner, Phys. Rev. Lett. **8**, 261 (1962).